Published in final edited form as:
Exp Eye Res. 2010 June ; 90(6): 771–779. doi:10.1016/j.exer.2010.03.013.

Chloride Channels and Transporters in Human Corneal Epithelium

Lin Cao[1,4], **Xiao-Dong Zhang**[2,4], **Xiaobo Liu**[4], **Tsung-Yu Chen**[2,4], and **Min Zhao**[1,3,4,*]

[1]Department of Dermatology, University of California, Davis, CA 95618, USA

[2]Department of Neurology, University of California, Davis, CA 95618, USA

[3]Department of Ophthalmology, University of California, Davis, CA 95618, USA

[4]Center for Neuroscience, University of California, Davis, CA 95618, USA

Abstract

Transport of water and electrolytes is critical for corneal clarity. Recent studies indicate another important function of transport of ions and electrolytes - establishing wound electric fields that guide cell migration. We found chloride (Cl^-) flux is a major component of the corneal wound electric current. In order to elucidate the mechanisms of Cl^- transport, we studied Cl^- channels and transporters in human corneal epithelial (HCE) cells.

We tested a transformed human corneal epithelial cell line (tHCE), primary cultures of human corneal epithelial cells (pHCE), and human donor corneas. We first used RT-PCR to determine expression levels of mRNA of CLC (Cl^- channel/transporter) family members and CFTR (cystic fibrosis transmembrane conductance regulator) in HCE cells. We then confirmed protein expression and distribution of selected CLC family members and CFTR with Western blot and immuno-fluorescence confocal microscopy. Finally, Cl^- currents were recorded with electrophysiological techniques.

The mRNAs of CLC-2, CLC-3, CLC-4, CLC-5, CLC-6, and CFTR were detected in the HCE cell line. CLC-1 and CLC-7 were not detectable. Western blot and immunostaining confirmed protein expression and distribution of CLC-2, CLC-3, CLC-4, CLC-6 and CFTR in human corneal epithelium. CLC-2 preferentially labeled the apical and basal layers, while CLC-3 and CLC-4 labeled only the superficial layer. CLC-6 and CFTR labeling showed a unique gradient with strong staining in apical layers which gradually decreased towards the basal layers. Corneal endothelium was positive for CLC-2, CLC-3, CLC-4, CLC-6 and possibly CFTR. Human corneal epithelial cells demonstrated voltage dependent Cl^- currents.

HCE cells express functional Cl^- channels and transporters. CLC-2, CLC-3, CLC-4, CLC-6, and CFTR had distinct expression patterns in human corneal epithelium. Those molecules and their distribution may play important roles in maintaining resting Cl^- fluxes and in regulating Cl^- flux at corneal wounds, which may be a major contributor to wound electrical signaling.

* Corresponding author: Min Zhao, Departments of Dermatology and Ophthalmology, School of Medicine, University of California, Davis, CA 95618, USA. Tel: 530 754 5129; Fax: 530 754 5136. minzhao@ucdavis.edu.

1. Introduction

Corneal epithelium and endothelium transport electrolytes and water between stroma, tear fluid and anterior aqueous chamber respectively. Corneal epithelium for example transports chloride (Cl^-) from the basal side to the tear side and sodium (Na^+) from the tear to the basal side (Candia, 2004; Fischbarg et al., 2006; Klyce and Crosson, 1985; Levin and Verkman, 2005; Reinach et al., 2008; Yang et al., 2000; Yang et al., 2001). One physiological role of such transport is to regulate corneal hydration – to maintain cornea deturgescence and therefore cornea clarity. Corneal endothelium transports Cl^-, which is required for fluid transport in rabbit corneal endothelium (Winkler *et al.*, 1992). Fluxes of Cl^- together with HCO_3^- and Na^+ generated osmotic gradients that drive water transport (Fischbarg, 1997). The cAMP and calcium-activated Cl^- transport was proposed to be essential for the HCO_3^-transport across the apical membrane of corneal endothelium from stroma into anterior chamber (Bonanno and Srinivas, 1997; Li *et al.*, 2008; Sun and Bonanno, 2002; Zhang *et al.*, 2006; Zhang *et al.*, 2002). In rabbit cornea, Cl^- flux accounted for 30% of water transport across corneal endothelium (Diecke *et al.*, 2007)

Accumulating experimental evidence suggest another important role for transport of electrolytes by corneal epithelium, namely to generate naturally-occurring electric fields (EFs) at corneal wounds (Chiang *et al.*, 1992; Nuccitelli, 2003; Reid *et al.*, 2007; Reid *et al.*, 2005). Several lines of evidence suggest that the endogenous wound EFs thus generated are powerful signals which can guide and stimulate corneal epithelial cells (CECs) to heal wounds (Chiang *et al.*, 1992; Jaffe, 1981; Jaffe and Vanable, 1984; McCaig *et al.*, 2005; Nuccitelli, 2003; Nuccitelli *et al.*, 2008; Reid *et al.*, 2007; Reid *et al.*, 2005; Sta Iglesia and Vanable, 1998; Zhao, 2009; Zhao *et al.*, 2006). Directional transport of ions (mainly Cl^- and Na^+) produces an electrical potential difference across the epithelium – which is called the transepithelial potential difference (TEP) (Barker *et al.*, 1982; Chiang *et al.*, 1992; Mukerjee *et al.*, 2006; Nuccitelli *et al.*, 2008; Sta Iglesia and Vanable, 1998). In frog and bovine corneas, active transport of ions results in a TEP of 25-45mV with the stromal side positive in relation to the tear side (Candia et al., 1968; Chiang et al., 1992; Fischer et al., 1972; Klyce, 1972). Injury collapses the TEP at the wound. The positive potential underneath the intact epithelium relative to the wound drives electric currents (by convention, the flow of positive charges) into the wound, resulting in endogenous EFs pointing to the wound center, the direction CECs migrate and proliferate to heal the wounds (Chiang *et al.*, 1992; Nuccitelli, 2003; Reid *et al.*, 2005; Zhao *et al.*, 2006).

Ion substitution and pharmacological stimulation suggest a major role for Cl^- in the wound currents. Cl^- free artificial tear solution (ATS) significantly increased transcorneal potential and the wound currents. Pharmacological agents that stimulate Cl^- transport, e.g. cyclic AMP mediated chloride channel activation, contributes to the generation of currents underlying the formation of EFs that promote cell migration (Levin et al., 2006; Reid et al., 2007; Reid et al., 2005; Zhao et al., 2006).

Several types of Cl^- transporting molecules have been found in CECs. Mouse, rabbit and human CECs express CFTR (cystic fibrosis transmembrane conductance regulator) and volume-regulated chloride channel (Al-Nakkash *et al.*, 2004; Al-Nakkash and Reinach, 2001; Levin and Verkman, 2006). Ca^{2+}-activated Cl^- channels CLCA2 was identified in human and chick CECs (Connon *et al.*, 2006; Itoh *et al.*, 2000). Rabbit CECs express RNAs encoding for CLC-2, CLC-3, CLC-5, CLC-6, CLC-7, but not for CLC-1 and CLC-4. Human CECs appear to express CLC-2 and CLC-3 (Davies et al., 2004). mRNAs for CLC-2, CLC-3, CLC-4, CLC-6, and CLC-7 were found in human CECs (Itoh *et al.*, 2000). Expression and asymmetric distribution is the basis of directional transport of ions. Using RT-PCR, Western blot and immunofluorescence microscopy, we examined the expression of chloride channels in primary,

transformed, and in situ corneal epithelial cells. We report here that human CECs express selective CLC family members, which have very distinct distribution in corneal epithelium.

2. Methods

2.1 PCR primers and antibodies

PCR primers for the chloride channels CLC-1 through CLC-7, CFTR and ANO1were designed using Primer3 online. CFTR regulates transcorneal potential and served as a positive control as it is expressed in human cornea (Levin *et al*., 2006; Zaidi *et al*., 2004). ANO1 or anoctamin 1 also known as TMEM16A, is a Ca^{2+} activated Cl^- channels in many transporting epithelia (Caputo et al., 2008; Schroeder et al., 2008; Yang et al., 2008). Tissue specific primers keratin 12, collagen 7 and collagen 8 were designed using the same protocols. Human CLC- mRNA sequences were downloaded from NCBI GenBank. A region that matched the consensus sequence for that CLC was chosen for PCR primers. At the same time the sequence was not in regions where the cDNA sequence was conserved between different members of the CLC family members. Primers were chosen to be 20 bp in length, with a GC content of 45-60%, no long repeats of a single base and 150 to 500 bp of products length. We further confirmed lack of cross-reactivity between the 3′ end of the CLC-primers and other known genes by BLAST searches. The optimized primer oligos used in the study are shown in Table 1. All primers were synthesized by Eurofins MWG Operon (UK).

Primary antibodies against CLC family members were from Santa Cruz (CA, USA): CLC-2 (Cat #: sc-16430 (C-20)), CLC-3 (Cat #: sc-17572 (K-17)), CLC-4 (Cat #: sc-16435(C-20)) and CLC-6 (Cat #: sc-16439 (N-20)). Primary antibodies against CFTR were from Cell Signaling (Cat #: CFTR 2269, USA).

2.2 Cell cultures and Donor corneas

SV40 transformed human corneal epithelial cells - tHCE cells were kindly provided by Dr Araki-Sasaki. They were cultured in supplemented hormonal epithelial medium (DMEM/F12) as previously described (Araki-Sasaki *et al.*, 1995; Zhao *et al.*, 1997). Once ~70% confluent, the cells were subcultured and medium was changed every 2 days. tsA201 cells (a subclone of HEK293 (Human Embryonic Kidney) cells) for negative control in electrophysiology experiments were cultured by using Dulbecco's Modified Eagle Medium supplemented with 20mM L-Glutamine,10% fetal bovine serum, 100 U/ml penicillin and 100 μg/ml streptomycin.

Primary culture of human corneal epithelial (pHCE) cells was described in details previously (Kahn et al., 1993). Donor corneas were placed epithelial-side up on a sterile surface and cut into ~12 triangular-shaped wedges. The corneal segments were then turned epithelial-side down in individual tissue culture wells and allowed to settle at room temperature for 20 minutes. One drop of serum-free medium (DMEM/F12 with antibiotic, human epidermal growth factor and insulin, Invitrogen, CA) was carefully placed upon each segment and the tissue was incubated overnight in a CO2 incubator (37°C, 5% CO_2). The next day, fresh medium was added. The medium was changed every 2 days until ~70% confluence, when the cells were subcultured into a fibronectin and collagen coated flask.

Use of human donor corneas from DCI Donor Services (Sacramento, CA, USA) for this research was approved by UC Davis Institutional Review Board (protocol number 200816682-1). Only corneas that were within 2 days from donors were used. No restrictions were placed on the age of the donor. Before shipping to our lab, the corneas were screened free of hepatitis B, hepatitis C, and HIV and stored in McCarey-Kaufman or Dexsol storage media at 4°C. We scored the corneas upon arrival. Only those corneas that were transparent with smooth surface were selected.

To collect fresh cornea epithelial cells from donor corneas, the epithelium was gently scraped off with a new blade under a dissecting microscope as described (Davies et al., 2004). The purity of freshly isolated epithelial cells and primary culture of corneal epithelial cells was confirmed with specific PCR primers Keratin12, Collagen 7, and Collagen 8.

2.3 RNA extraction and RT-PCR (reverse transcription polymerase chain reaction)

tHCE (1×10^6) were mixed with 1 ml of TriZol reagent (Invitrogen, UK). RNA was then extracted following the manufacturer's protocol, followed by DNase treatment, phenol-chloroform extraction, and ethanol precipitation. RNA was re-suspended in 30 μl RNase free water, analyzed by agarose gel electrophoresis and quantified by spectrophotometry (absorbance at 260 nm).

RNA (2 μg) from HCE cells was heated to denature at 65 °C f or 5 min, cooled 1 min on ice and reverse transcribed in a 20 μl reaction solution containing 2.5 μM oligo $(dT)_{20}$ primer, 1× RT buffer, 0.5 mM each dNTP, 5 mM dithiothreitol, 40 U RNase-OUT and 200 U Superscript II reverse transcriptase (Invitrogen, UK). The cDNA synthesis was carried out at 50 °C for 50 min and 1 μl RNase H was added for removing RNA. PCR was then performed in 30 μl reaction volumes containing 2 μl of undiluted cDNA, 1× PCR buffer, 1.5 mM $MgCl_2$, 0.2 mM each dNTP, 0.5 μM each primer, and 2.5 U Taq polymerase (Invitrogen, UK). After 35 cycles of 94 °C for 1 min, annealing temperature for 1 min, and 72 °C for 1 min, the products were evaluated on a 2% agarose gel. Triplicate PCR experiments were done to confirm the results. Each experiment used RNA originating from a different batch of cell sample.

2.4 Protein extraction and Western blot

tHCE Cells ($\sim5\times10^6$) or pHCE cells and human corneal epithelium tissue were collected and rinsed with cold D-PBS and snap frozen in liquid nitrogen for further use. Non-ocular tissues (mouse muscle and brain) were collected from fresh carcasses for other experimental purpose without pharmacological treatment. The tissue was rinsed in D-PBS and snap frozen in liquid nitrogen until use. All samples were lysed with lysis buffer (10 mM Tris-HCL, 50 mM NaCl, 5 mM EDTA, 50 mM sodium fluoride, 1% Triton X-100, 30 mM $Na_4P_2O_7$ 1 mM sodium orthovanadate and protease inhibitor cocktail) (Boehringer-Ingelheim, Ingelheim, Germany). Equal amounts of protein lysate (50μg) were loaded onto 4 to 10% Bis-Tris gel, followed by electroblot analysis onto nitrocellulose membrane (Invitrogen, UK). The membranes were stained with Ponceau S for detection of transfer efficiency, then were blocked with 5% milk TBST (pH 7.4 with 0.1% (w/v) Tween 20) for 2 h. The membrane was incubated with relevant primary antibodies respectively (1:100 dilution of anti-CLC-2, and CLC-4, from Santa Cruze, CA, USA) 1:1000 dilution of anti-CFTR (Cell Signaling, USA) or anti-tubulin (Sigma-Aldrich, UK) overnight at 4°C. Anti-rabbit/mouse/goat secondary antibody with horseradish peroxidase (1:5000) was used, and the immunoblots were detected by an enhanced chemiluminescence (ECL) detection system (Amersham Pharmacia Biotech, UK). The western blotting was repeated more than three times.

2.5 Immunofluorescence microscopy

Human donor corneas were used within 48h of death. The corneas were fixed with 4% paraformaldehyde in PBS for 20 min. The samples were frozen at -80C°, and sections were obtained by slicing the samples (sliding arc CO_2 freezing microtome) (Leitz, Inc., Rockleigh, N J) and collecting them in sodium azide. Cryosections (10-15 μm thick) were cut and collected on gelatin coated slides. Nonspecific binding sites were blocked with PBS containing 2% bovine serum albumin (BSA) plus 0.3% Triton X-100, for 30 min at room temperature. Primary antibodies, diluted 1:200 in 1% BSA-PBS and 0.3% Triton X-100 were applied to corneal sections overnight at 4°C in a m oist chamber. After several washes in PBS, the tissue sections were labeled with cy3 conjugated secondary antibody (Molecular Probes) diluted 1:500, for 1

h at room temperature and mounted with Vectorshield mounting medium with DAPI (Vector Labs, Peterborough, UK). Fluorescent signals were visualized on a Zeiss LSM 510 META Confocal microscope using 20×/0.5w and 40×/1.2w objectives.

2.6 Image analysis

Fluorescence intensity was measured using MetaMorph software (Universal Imaging Corp.). A very thick line (~ a cell in width) was drawn perpendicular to the epithelial surface and across the corneal epithelium. Fluorescence intensity along the line was recorded. One additional method was used to quantify fluorescence intensity in apical layers, middle layers and basal layers. A rectangle of three cells-long and two cells-width was drawn in the apical layers, middle layers and basal layers. After background (no tissue area) subtraction, the fluorescence intensity of CLC6 and CFTR staining was normalized against actin filament staining. Three areas of each section and three sections from each donor cornea were quantified. The fluorescence intensity was averaged from three donor corneas. Those semi-quantitative data were statistically compared using unpaired two-tailed Student's *t* test.

2.7 Electrophysiology

Whole-cell current recordings from HCE cells were performed using an Axopatch 200B amplifier (Axon Instrument/Molecular Devices, Union City, CA). Currents were digitally filtered at 1 kHz and digitized at 2 kHz using a Digidata 1322A digitizer and pClamp 9.0 software (Axon Instrument/Molecular Devices). The recording pipettes were pulled from borosilicate glass (World Precision Instruments, Sarasota, FL) using a PP-830 pipette puller PP-830 (Narishige International, Inc., New York, NY), and the pipette resistance was ~ 2-3 MΩ when filled with the pipette solution. The pipette solution contained (in mM): 110 Na Glutamate, 30 NaCl, 5 $MgSO_4$, 10 HEPES, 1 EGTA, pH 7.4; the standard bath solution contained (in mM): 140 TEACl, 1$MgCl_2$, 10 Hepes, pH=7.4. The low chloride bath solution is the same as the pipette solution. All experiments were conducted at room temperature and the recording was repeated in 4 cells (n=4).

3. Results

3.1 Expression of CLC mRNA

We designed a set of PCR primers that would amplify each member of the CLC family based on human gene sequence (Table 1). The panel of primers was used to evaluate the CLC gene expression profile of the HCE cells. Due to freshness of tissue, we only tested the tHCE. BLAST hit was scored to confirm that the primers amplified the expected CLC product. We also used mock reverse transcription reactions, used as a negative control to exclude genomic DNA contamination of mRNA samples. The majority of CLC mRNAs were found to be expressed in HCE cells, including mRNAs for CLC-2, CLC-3, CLC-4, CLC-5, whereas CLC-6, CLC-1 and CLC-7 were not detected (Fig. 1). mRNAs for other two molecules CFTR and ANO1 also exist in the tHCE cells. As a control the kidney specific channel, CLC-Kb was not found in tHCE cells.

3.2 Expression of CLC proteins

To determine whether the mRNAs identified above are indeed translated into proteins, we used Western blot to determine protein expression of CLC-2, CLC-4 and CFTR in freshly isolated HCE tissues, pHCE cells and tHCE cells. Western blot of all three proteins confirmed their expression (Fig. 2). One unexpected result was that proteins of CLC-2, CLC-4 and CFTR were expressed at significantly higher level in freshly isolated HCE tissues than in cultured epithelial cells (primary culture or cell line). tHCE cells expressed very low levels of these three proteins. Nevertheless, careful examination revealed the presence of positive bands, which was

confirmed in three separate experiments, and by increasing the total amount of protein loaded. The difference in expression level may have significant functional implications - the expression of CLC-s is regulated during stratification and has functional significance at the tissue level.

3.3 Distinct distribution of CLCs in human corneal epithelium

We next examined the distribution of CLCs in corneal epithelium. Polarized distribution of channels and pumps underlies directional absorption and secretion. In polarized kidney epithelium for example, ion transporters and pumps are distributed asymmetrically. One striking result of our study is that CLCs have very distinct distribution pattern (Fig. 3). The unique distribution of CLC-2, CLC-3, CLC-4, CLC-6 and CFTR strongly suggests directional and regulated transport of Cl^- across human corneal epithelium.

We found three different patterns of distribution of CLC and CFTR in human corneal epithelium: 1) expression on the apical and basal layers; 2) expression only on the apical layers; 3) a gradient expression with highest expression level in the apical layers.

CLC-2 was distributed in both the apical layer and basal layer (Fig. 3A). In HCE cells in the superficial layer, CLC-2 staining was restricted to the apical side. In the basal cells, CLC-2 staining was restricted to the stromal side. This is better appreciated in the merged image combining epithelial nuclear and CLC-2 staining to show the whole epithelial structure (Fig. 3A, right panel).

CLC-3 and CLC-4 were expressed exclusively in superficial layer epithelial cells (Fig. 3B, C). In positive cells, CLC-3 and CLC-4 staining was restricted to the apical side. CLC-6 and CFTR showed a different type of distribution: a gradient with highest expression in the apical squamous cell layers, but they were also expressed in wing cells and basal cells with gradually and markedly decreased level (Fig. 3D, E). Quantitative analyses confirmed the gradient distribution (Fig. 4). While CLC-2, CLC-3, CLC-4 and CLC-6 were detected mainly on the cell membranes or cell periphery, CFTR was present more homogenously in the cytoplasm (Fig. 3E).

3.4 Distribution of CLCs in human corneal endothelium

There were few CLC-2 and CLC-6 positive cells in the stroma. Cells positive for CLC-3 and CLC-4 were even sparser in the stroma and stained weaker compared to CLC-2 and CLC-6 (data not shown). Human cornea endothelial cells were stained positive for CLC-2, CLC-3, CLC-4, CLC-6 and CFTR (Fig. 5). CLC-2 was preferentially distributed in the apical side of the endothelial layer (Fig. 5A), whereas CLC-3, CLC-4 and CLC-6 were distributed throughout the whole endothelial layer with a tendency biased to the stromal side (Fig. 5B, C, D). Staining of CFTR was on the basal side and very weak (Fig. 5E). Increasing the detection sensitivity showed the autofluorescence of Descemet's membrane (Fig. 5E, thick red staining just beneath the endothelial layer). Control staining using isoform IgG as primary antibodies or omission of primary antibodies showed no staining of CLC-2, CLC-3, CLC-4, CLC-6 and CFTR (data not shown).

3.5 Chloride currents recorded in HCE cells

To confirm the functionality of chloride channels and transporters, whole-cell chloride currents were recorded from the pHCE and tHCE. As a control, whole-cell recording was also performed on tsA201 cells under the same recording condition. tsA201 cells are a HEK293 (Human Embryonic Kidney) cell subclone. Previous elegant studies have demonstrated Cl^- currents in rabbit corneal epithelial cells (Al-Nakkash et al., 2004; Al-Nakkash and Reinach, 2001). We confirmed that human CECs had Cl^- currents. Whole-cell currents were measured by clamping the membrane potential from +80 to -120 mV in 20 mV increments with a holding potential

of 0 mV. As shown in Fig. 6, outwardly rectifying chloride currents were recorded from both the pHCE (Fig. 6A, left) and tHCE cells (Fig. 6B, left), but not from tsA201 control cells (Fig. 6C, left). The currents from the pHCE and tHCE cells were dependent on the extracellular chloride concentrations. When the chloride concentration in the bath solution was reduced to 30 mM, the outward currents were reduced (Fig. 6A & B, middle) and the reversal potential was shifted to the right, approaching 0 mV as indicated by the steady state current-voltage relationships (Fig. 6A & B, right). This shift did not occur in the control cells (Fig. 6C, right). We found that the chloride currents in pHCE and tHCE cells were very similar (comparing Fig. 6A with Fig. 6B). To characterize the currents, we calculated the rectification index of the currents by dividing the absolute current at -120 mV by the current at +80mV. We obtained indices of 0.45 ± 0.03 for the pHCE cells and 0.40 ± 0.07 for tHCE cells. However, the index was 1.28 ± 0.09 for tsA201cells. This demonstrated the specificity of the Cl^- currents in cornea epithelial cells.

4. Discussion

The molecular mechanisms of the EFs at corneal wounds are poorly understood. Our previous studies suggested a significant role for Cl^- flux . We therefore sought to determine Cl^- channels in HCE cells. We report here that: 1) tHCE cells express mRNAs of CLC-2, CLC-3, CLC-4, CLC-5, CLC-6, CFTR, and ANO1 (or TMEM16A); 2) culturing CECs appears to reduce the protein levels of CLC-2, CLC-4 and CFTR; 3) CLC-2, CLC-3, CLC-4, CLC-6 and CFTR are expressed differentially in the different layers of corneal epithelium; 4) both pHCE and tHCE cells have functional chloride currents.

4.1 Expression of CLCs

Rabbit CECs express RNAs encoding for CLC-2, CLC-3, CLC-5, CLC-6, CLC-7, but not CLC-1 and CLC-4 (Davies et al., 2004). In the present study we focused on seven members of the CLC channel/transporter family (CLC-1, CLC-2, CLC-3, CLC-4, CLC-5, CLC-6, CLC-7). mRNAs encoding for CLC-2, CLC-3, CLC-4, CLC-5, and CLC-6, CFTR and ANO1 are expressed in HCE cells (Fig. 1). Expression of CLC-2, CLC-3, CLC-4, CLC-6 and CFTR in HCE cells was confirmed with RT-PCR, Western blot and immunofluorescence staining (Figs.1, 2, 3). Human corneal endothelium was also positively labelled with CLC-2, CLC-3, CLC-4, CLC-6 and CFTR antibodies (Fig. 5). Expression of CLC-4, but not CLC-6 and CLC-7 in human CECs, while rabbit CECs do not express CLC-4, but CLC-5 and CLC-7 may suggest interspecies difference in expression of CLC chloride channels and transporters.

Another important finding is that stratified corneal epithelial tissue harvested directly from donor corneas showed higher protein expression levels of CLC-2, CLC-4 and CFTR (the only proteins we probed with Western blotting). Stratification of chick corneal epithelium during development and stratification of human CECs cultured on amniotic membrane is accompanied by significant changes in CLCA2 expression. In monolayer culture, human CECs express relatively little CLCA2. However, as the number of cell-layers increases, the gene expression level and protein staining intensity of CLCA2 increase, mainly within the basal cells (Connon *et al*., 2006). Further investigation of the expression level during stratification may offer insights into the whole epithelium as a transporting unit.

4.2 Distribution of CLCs

In order to carry out directional transepithelial secretion and absorption, ion transporting molecules are distributed in a tightly controlled manner in polarized epithelia. One significant finding of our current research is the distinct distribution of CLC-2, CLC-3, CLC-4, CLC-6 and CFTR in human corneal epithelium. CLC-2 distribution is similar to what has been reported in rabbit corneal epithelium – i.e. restricted to the apical and basal layers (Fig. 3). Distribution

of CLC-3, CLC-4, CLC-6 and CFTR in human corneal epithelium has not been reported before. CLC-3 and CLC-4 are exclusively located in the apical layers (Fig. 3B, C). A noticeable difference is the apical membrane expression of CLC-3 and CLC-4. A significant proportion of CLC-3 is expressed intracellularly in rabbit corneal epithelial cells (Davies *et al.*, 2004). CLC-6 and CFTR have another type of distribution – their expression levels are higher in the apical layers and gradually decreased towards the basal layers (Fig. 3D, E;Fig. 4). Another family of Cl^- channels, calcium-activated chloride channels, are distributed asymmetrically in the basal layer of the corneal epithelium (Connon *et al.*, 2006;Davies *et al.*, 2004). This polarized distribution suggests a structural basis of directional Cl^- transport in the corneal epithelium.

4.3 CLC channels and transporters in stroma and endothelium

mRNA and protein of CLC-2 and CLC-3 were detected in rabbit corneal stroma and human endothelium (Davies et al., 2004; Sun et al., 2001). Our immunofluorescence staining showed CLC-2, 3, 4, and 6 positive cells in stroma and corneal endothelial cells. In the stroma, more cells appeared to be positive for CLC-2 and CLC-6. Human corneal endothelial cells are positive for CLC-2, 3, 4, 6, and possibly CFTR (Fig. 5). This is similar to what has been reported for rabbit corneal endothelium, which are positive for CLC-2 and CLC-4 (Davies *et al.*, 2004). CFTR staining was very weak in endothelial cells. Increasing the gain of the confocal microscope revealed patchy staining of the basal membrane, however this was confounded by the autofluorescence of the Descemet's membrane (Fig. 5E).

4.4 Chloride channels in human CECs

Similar Cl^- currents were recorded from the primary and transformed human CECs (Fig. 6), whereas the western blotting showed marked differences in the levels of CLC-2, CLC-4 and CFTR between the primary and transformed human CECs. The currents are unlikely to be CLC-2 currents due to the outward rectifying behavior recorded. It is also not likely to be mediated by CFTR as our recording solution significantly dilutes intracellular protein kinases and ATP which are required for CFTR activation. Even though the Western blotting showed different expression levels of CLC-2 and CFTR between primary and transformed HCE cells, the recorded currents are actually similar. The Cl^- currents could be a combination of currents from CLCs, Ca^{2+} activated Cl^- channels, and volume regulated Cl^- channels. Volume-regulated anion channels were characterized in SV40-immortalized rabbit corneal epithelial cells (Al-Nakkash et al., 2004;Reinach et al., 2008). Those channels mediate a robust regulatory volume decrease response to a hypotonic challenge. However, the cells did not show Cl^- current in isotonic solution (Al-Nakkash *et al.*, 2004). Isotonic solution and Ca^{2+} free recording conditions minimized the involvement of volume regulated Cl^- channels and Ca^{2+} activated Cl^- channels. Further experiments are needed to determine specifically the molecular participants of the recorded Cl^- currents in HCE cells (Fig. 6).

In conclusion, using immunostaining, confocal microscopy, electrophysiology and molecular techniques, we investigated CLCs in HCE cells. We established expression profiles and distribution of CLCs. HCE cells express multiple Cl^- channels. Corneal epithelial tissue expresses much higher levels of CLC-2, CLC-4, and CFTR than cultured cells. CLC-2, CLC-3, CLC-4, CLC-6 and CFTR had distinct expression pattern in human corneal epithelium. Furthermore, we confirmed Cl^- currents in human corneal epithelial cells. The expression pattern suggests different functional roles for CLCs. Our results suggest that transport of Cl^- in HCE cells may play important roles in maintaining resting Cl^- fluxes in intact cornea and increased Cl^- flux at corneal wounds, which could be a major contributor for wound electrical signaling. Further study to elucidate the regulation of expression and distribution of CLCs at corneal wounds will offer novel insights into ion fluxes and their role in corneal wound healing.

Acknowledgments

This work is supported by NIH 1R01EY019101. MZ is also supported by grants from California Institute of Regenerative Medicine RB1-01417, NSF MCB-0951199, UC Davis Dermatology Developmental Fund. We thank Dr. Brian Reid for English correction and Xiaohong Fan for helping with Western blot.

References

Al-Nakkash L, Iserovich P, Coca-Prados M, Yang H, Reinach PS. Functional and molecular characterization of a volume-activated chloride channel in rabbit corneal epithelial cells. The Journal of membrane biology 2004;201:41–49. [PubMed: 15635811]

Al-Nakkash L, Reinach PS. Activation of a CFTR-mediated chloride current in a rabbit corneal epithelial cell line. Investigative ophthalmology & visual science 2001;42:2364–2370. [PubMed: 11527951]

Araki-Sasaki K, Ohashi Y, Sasabe T, Hayashi K, Watanabe H, Tano Y, Handa H. An SV40-immortalized human corneal epithelial cell line and its characterization. Invest Ophthalmol Vis Sci 1995;36:614–621. [PubMed: 7534282]

Barker AT, Jaffe LF, Vanable JW Jr. The glabrous epidermis of cavies contains a powerful battery. Am J Physiol 1982;242:R358–366. [PubMed: 7065232]

Bonanno JA, Srinivas SP. Cyclic AMP activates anion channels in cultured bovine corneal endothelial cells. Experimental eye research 1997;64:953–962. [PubMed: 9301476]

Candia OA. Electrolyte and fluid transport across corneal, conjunctival and lens epithelia. Exp Eye Res 2004;78:527–535. [PubMed: 15106931]

Candia OA, Zadunaisky JA, Bajandas F. Electrical potential profile of the isolated frog cornea. Invest Ophthalmol 1968;7:405–415. [PubMed: 5663551]

Caputo, A.; Caci, E.; Ferrera, L.; Pedemonte, N.; Barsanti, C.; Sondo, E.; Pfeffer, U.; Ravazzolo, R.; Zegarra-Moran, O.; Galietta, LJ. Science. Vol. 322. New York, N.Y: 2008. TMEM16A, a membrane protein associated with calcium-dependent chloride channel activity; p. 590-594.

Chiang M, Robinson KR, Vanable JW Jr. Electrical fields in the vicinity of epithelial wounds in the isolated bovine eye. Experimental eye research 1992;54:999–1003. [PubMed: 1521590]

Connon C, Kawasaki S, Liles M, Koizumi N, Yamasaki K, Nakamura T, Quantock A, Kinoshita S. Gene expression and immunolocalisation of a calcium-activated chloride channel during the stratification of cultivated and developing corneal epithelium. Cell and Tissue Research 2006;323:177–182. [PubMed: 16158324]

Davies N, Akhtar S, Turner HC, Candia OA, To CH, Guggenheim JA. Chloride channel gene expression in the rabbit cornea. Molecular vision 2004;10:1028–1037. [PubMed: 15635293]

Diecke FP, Ma L, Iserovich P, Fischbarg J. Corneal endothelium transports fluid in the absence of net solute transport. Biochimica et biophysica acta 2007;1768:2043–2048. [PubMed: 17597578]

Fischbarg J. Mechanism of fluid transport across corneal endothelium and other epithelial layers: a possible explanation based on cyclic cell volume regulatory changes. The British journal of ophthalmology 1997;81:85–89. [PubMed: 9135416]

Fischbarg J, Diecke FP, Iserovich P, Rubashkin A. The Role of the Tight Junction in Paracellular Fluid Transport across Corneal Endothelium. Electro-osmosis as a Driving Force. J Membr Biol 2006;210:117–130. [PubMed: 16868674]

Fischer F, Voigt G, Liegl O, Wiederholt M. Potential difference and short-circuit current in isolated human cornea. Pflugers Arch 332, Suppl 1972;332:R391.

Itoh R, Kawamoto S, Miyamoto Y, Kinoshita S, Okubo K. Isolation and characterization of a Ca(2+)-activated chloride channel from human corneal epithelium. Current eye research 2000;21:918–925. [PubMed: 11262615]

Jaffe LF. Control of development by steady ionic currents. Federation proceedings 1981;40:125–127. [PubMed: 7193143]

Jaffe LF, Vanable JW Jr. Electric fields and wound healing. Clin Dermatol 1984;2:34–44. [PubMed: 6336255]

Kahn CR, Young E, Lee IH, Rhim JS. Human corneal epithelial primary cultures and cell lines with extended life span: in vitro model for ocular studies. Invest Ophthalmol Vis Sci 1993;34:3429–3441. [PubMed: 7693609]

Klyce SD. Electrical profiles in the corneal epithelium. J Physiol 1972;226:407–429. [PubMed: 4538944]

Klyce SD, Crosson CE. Transport processes across the rabbit corneal epithelium: a review. Curr Eye Res 1985;4:323–331. [PubMed: 3893897]

Levin MH, Kim JK, Hu J, Verkman AS. Potential difference measurements of ocular surface Na+ absorption analyzed using an electrokinetic model. Invest Ophthalmol Vis Sci 2006;47:306–316. [PubMed: 16384978]

Levin MH, Verkman AS. CFTR-regulated chloride transport at the ocular surface in living mice measured by potential differences. Invest Ophthalmol Vis Sci 2005;46:1428–1434. [PubMed: 15790911]

Levin MH, Verkman AS. Aquaporins and CFTR in ocular epithelial fluid transport. J Membr Biol 2006;210:105–115. [PubMed: 16868675]

Li J, Allen KT, Sun XC, Cui M, Bonanno JA. Dependence of cAMP meditated increases in Cl- and HCO (3)- permeability on CFTR in bovine corneal endothelial cells. Experimental eye research 2008;86:684–690. [PubMed: 18325495]

McCaig CD, Rajnicek AM, Song B, Zhao M. Controlling cell behavior electrically: current views and future potential. Physiol Rev 2005;85:943–978. [PubMed: 15987799]

Mukerjee EV, Isseroff RR, Nuccitelli R, Collins SD, Smith RL. Microneedle array for measuring wound generated electric fields. Conf Proc IEEE Eng Med Biol Soc 2006;1:4326–4328. [PubMed: 17947077]

Nuccitelli R. A role for endogenous electric fields in wound healing. Curr Top Dev Biol 2003;58:1–26. [PubMed: 14711011]

Nuccitelli R, Nuccitelli P, Ramlatchan S, Sanger R, Smith PJ. Imaging the electric field associated with mouse and human skin wounds. Wound Repair Regen 2008;16:432–441. [PubMed: 18471262]

Reid B, Nuccitelli R, Zhao M. Non-invasive measurement of bioelectric currents with a vibrating probe. Nat Protoc 2007;2:661–669. [PubMed: 17406628]

Reid B, Song B, McCaig CD, Zhao M. Wound healing in rat cornea: the role of electric currents. FASEB J 2005;19:379–386. [PubMed: 15746181]

Reinach, PS.; Capó-Aponte, JE.; Mergler, S.; Pokorny, KS. Roles of Corneal Epithelial Ion Transport Mechanisms in Mediating Responses to Cytokines and Osmotic Stress. Humana Press; Totowa, NJ: 2008.

Schroeder BC, Cheng T, Jan YN, Jan LY. Expression cloning of TMEM16A as a calcium-activated chloride channel subunit. Cell 2008;134:1019–1029. [PubMed: 18805094]

Sta Iglesia DD, Vanable JW Jr. Endogenous lateral electric fields around bovine corneal lesions are necessary for and can enhance normal rates of wound healing. Wound Repair Regen 1998;6:531–542. [PubMed: 9893173]

Sun XC, Bonanno JA. Expression, localization, and functional evaluation of CFTR in bovine corneal endothelial cells. American journal of physiology 2002;282:C673–683. [PubMed: 11880256]

Sun XC, McCutheon C, Bertram P, Xie Q, Bonanno JA. Studies on the expression of mRNA for anion transport related proteins in corneal endothelial cells. Curr Eye Res 2001;22:1–7. [PubMed: 11402373]

Winkler BS, Riley MV, Peters MI, Williams FJ. Chloride is required for fluid transport by the rabbit corneal endothelium. The American journal of physiology 1992;262:C1167–1174. [PubMed: 1590358]

Yang H, Reinach PS, Koniarek JP, Wang Z, Iserovich P, Fischbarg J. Fluid transport by cultured corneal epithelial cell layers. The British journal of ophthalmology 2000;84:199–204. [PubMed: 10655198]

Yang H, Wang Z, Miyamoto Y, Reinach PS. Cell signaling pathways mediating epidermal growth factor stimulation of Na:K:2Cl cotransport activity in rabbit corneal epithelial cells. The Journal of membrane biology 2001;183:93–101. [PubMed: 11562791]

Yang YD, Cho H, Koo JY, Tak MH, Cho Y, Shim WS, Park SP, Lee J, Lee B, Kim BM, Raouf R, Shin YK, Oh U. TMEM16A confers receptor-activated calcium-dependent chloride conductance. Nature 2008;455:1210–1215. [PubMed: 18724360]

Zaidi T, Mowrey-McKee M, Pier GB. Hypoxia increases corneal cell expression of CFTR leading to increased Pseudomonas aeruginosa binding, internalization, and initiation of inflammation. Investigative ophthalmology & visual science 2004;45:4066–4074. [PubMed: 15505057]

Zhang Y, Li J, Xie Q, Bonanno JA. Molecular expression and functional involvement of the bovine calcium-activated chloride channel 1 (bCLCA1) in apical HCO3- permeability of bovine corneal endothelium. Experimental eye research 2006;83:1215–1224. [PubMed: 16899243]

Zhang Y, Xie Q, Sun XC, Bonanno JA. Enhancement of HCO(3)(-) permeability across the apical membrane of bovine corneal endothelium by multiple signaling pathways. Invest Ophthalmol Vis Sci 2002;43:1146–1153. [PubMed: 11923259]

Zhao M. Electrical fields in wound healing-An overriding signal that directs cell migration. Semin Cell Dev Biol 2009;20:674–682. [PubMed: 19146969]

Zhao M, McCaig CD, Agius-Fernandez A, Forrester JV, Araki-Sasaki K. Human corneal epithelial cells reorient and migrate cathodally in a small applied electric field. Curr Eye Res 1997;16:973–984. [PubMed: 9330848]

Zhao M, Song B, Pu J, Wada T, Reid B, Tai G, Wang F, Guo A, Walczysko P, Gu Y, Sasaki T, Suzuki A, Forrester JV, Bourne HR, Devreotes PN, McCaig CD, Penninger JM. Electrical signals control wound healing through phosphatidylinositol-3-OH kinase-gamma and PTEN. Nature 2006;442:457–460. [PubMed: 16871217]

Abbreviations

CLC	chloride channels and transporters of CLC gene family
EF	electric fields
HCE	human corneal epithelial
tHCE	transformed corneal epithelial cells
pHCE	primary human corneal epithelial cells
CEC	corneal epithelial cell
CFTR	cystic fibrosis transmembrane conductance regulator
NKCC	Na:K:2Cl cotransporter
EGF	epidermal growth factor
ANO1	or anoctamin 1 is a calcium activated chloride channel also known as TMEM16A

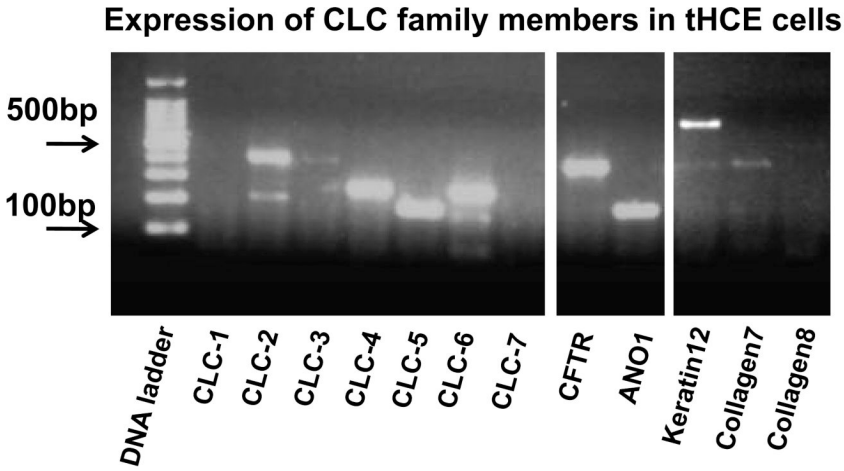

Figure 1. RT-PCR products for CLCs from human corneal epithelial cells

Transformed human corneal epithelial cell samples (tHCE) were used. DNA ladder is on the left. Tissue specific markers are on the right.

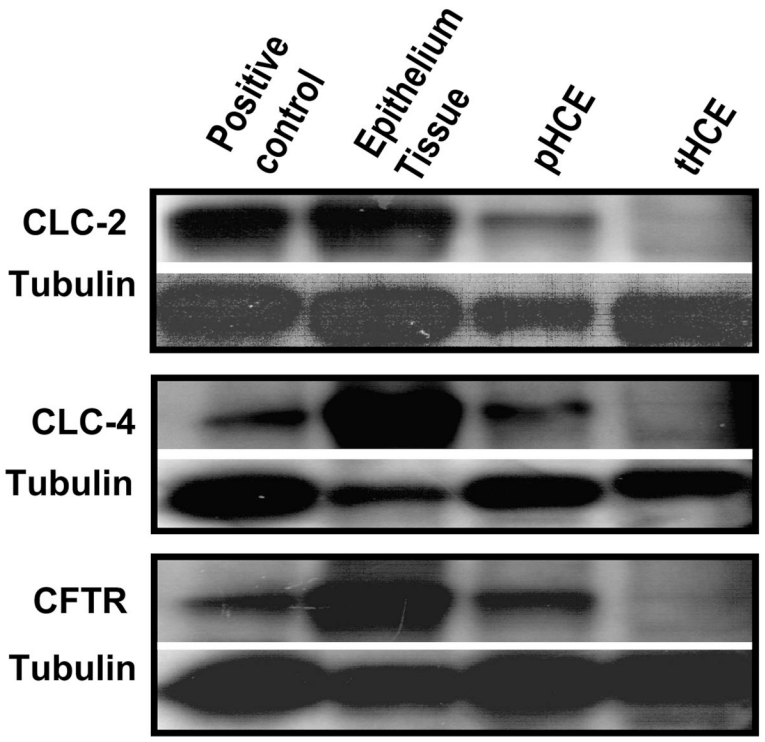

Figure 2. Western blot confirmed expression of proteins of CLC family members in human corneal epithelial cells

Human corneal epithelial tissue, primary cultured human corneal epithelial cells and transformed human corneal epithelial cells were probed with specific antibodies against CLC-2, CLC-4, and CFTR. Mouse heart tissue was used as positive control for CLC-2, mouse brain tissue was used as positive control for CLC-4 and CFTR. Tubulin was used as a loading control. Because of the variation in the expression level of target proteins, we varied loading quantity significantly.

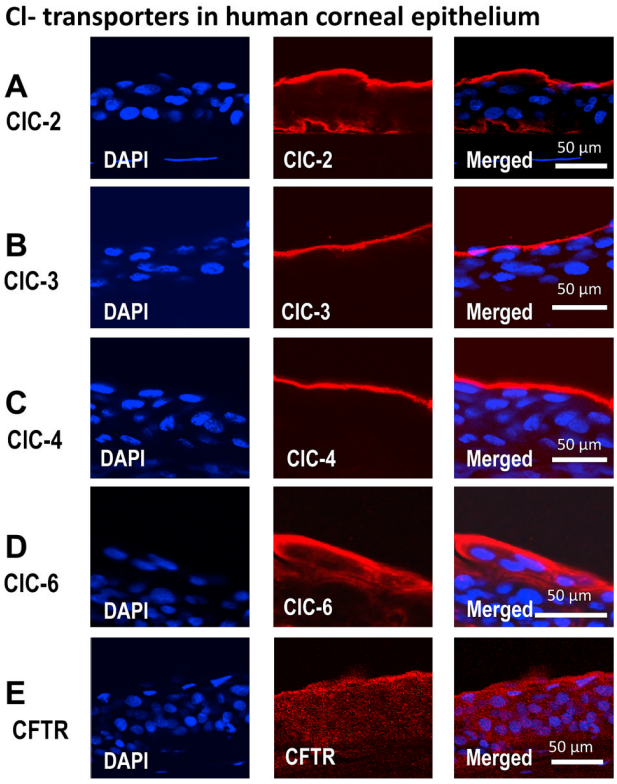

Figure 3. Confocal images of immunofluorescence staining for CLC family members in human corneal epithelium

CLC family members CLC-2, CLC-3, CLC-4, CLC-6 and CFTR show distinct distribution in human corneal epithelium. Actin (not show here) and DAPI (for nuclear staining) were used as controls. (A), CLC-2 is distributed at the apical and basal layers of corneal epithelium. (B) and (C), CLC-3, and CLC-4 are expressed at the apical layer. (D) and (E), CLC-6 and CFTR expressed preferentially at the apical layers with expression level gradually decreasing towards the basal layer. Tear side is orientated to the top and basal side towards the bottom.

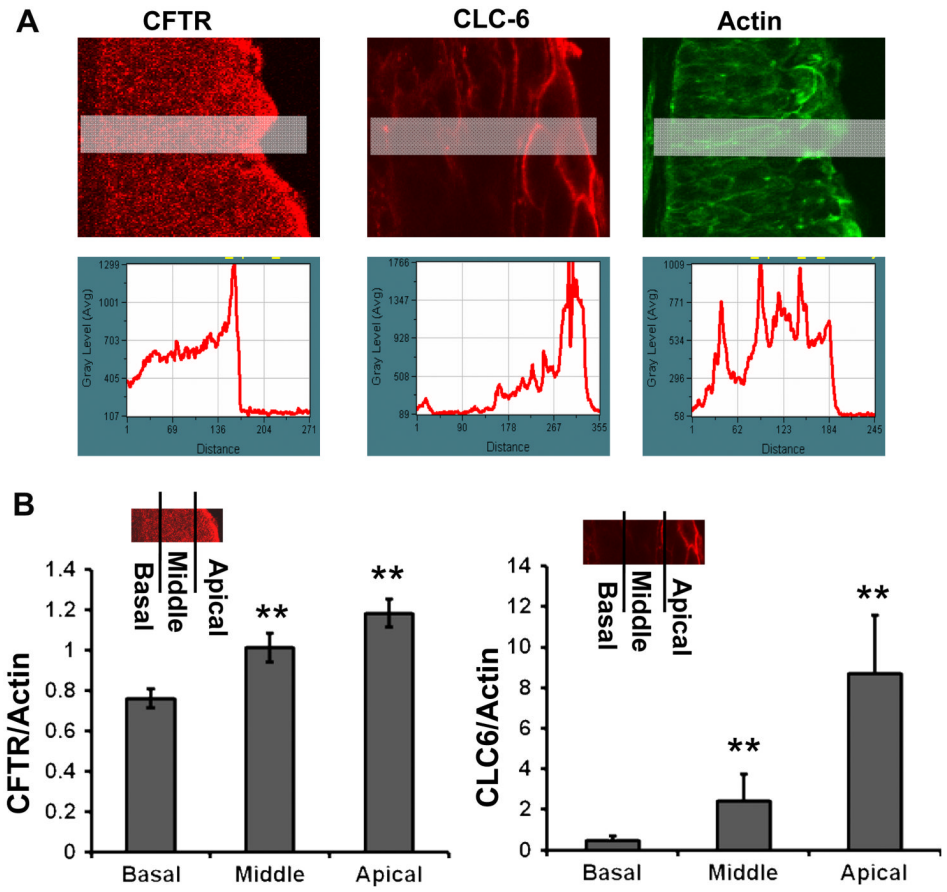

Figure 4. Gradients of CLC6 and CFTR staining in human corneal epithelium

Quantitative analyses were performed with Metamorph software. (A) Fluorescence intensity along the shaded rectangles is shown in the corresponding line graph below. Actin filament staining is used as an internal control. (B) The fluorescence intensity of CFTR and CLC-6 in the apical, middle and basal layers of corneal epithelium was significantly different from each other. Apical layers show strongest staining, which gradually decreased towards the basal layers. The fluorescence intensity of CFTR and CLC-6 staining was normalized using the fluorescence value of actin filaments. ** P<0.01.

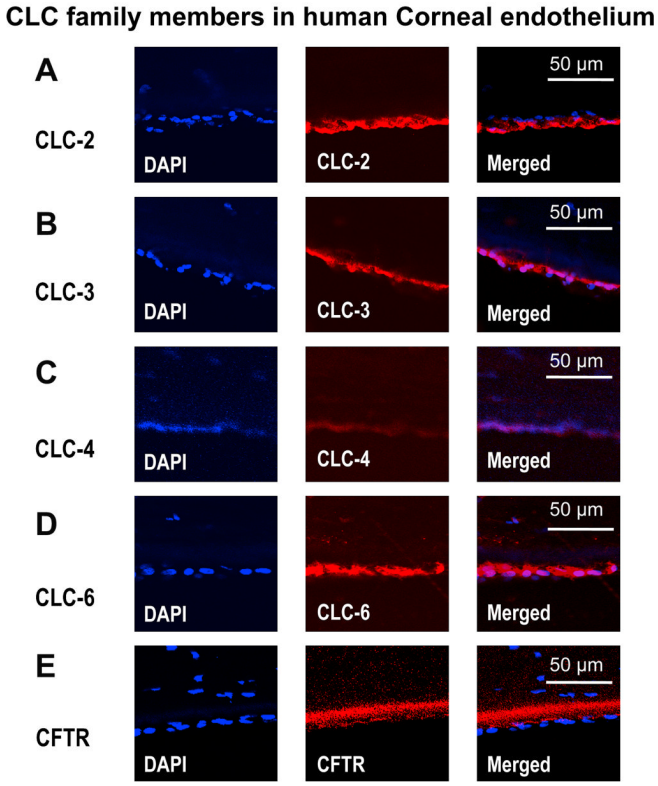

Figure 5. Confocal images of immunofluorescence staining for CLC family members in human corneal endothelium

Human corneal endothelial cells are positive for immunostaining of CLC family members CLC-2, CLC-3, CLC-4, CLC-6 and CFTR. DAPI (for nuclear) staining was used to show the endothelium. Control staining using isoform IgG, or omission of the primary antibodies showed no staining (not show here). Stromal side is orientated to the top and apical side is orientated towards the bottom.

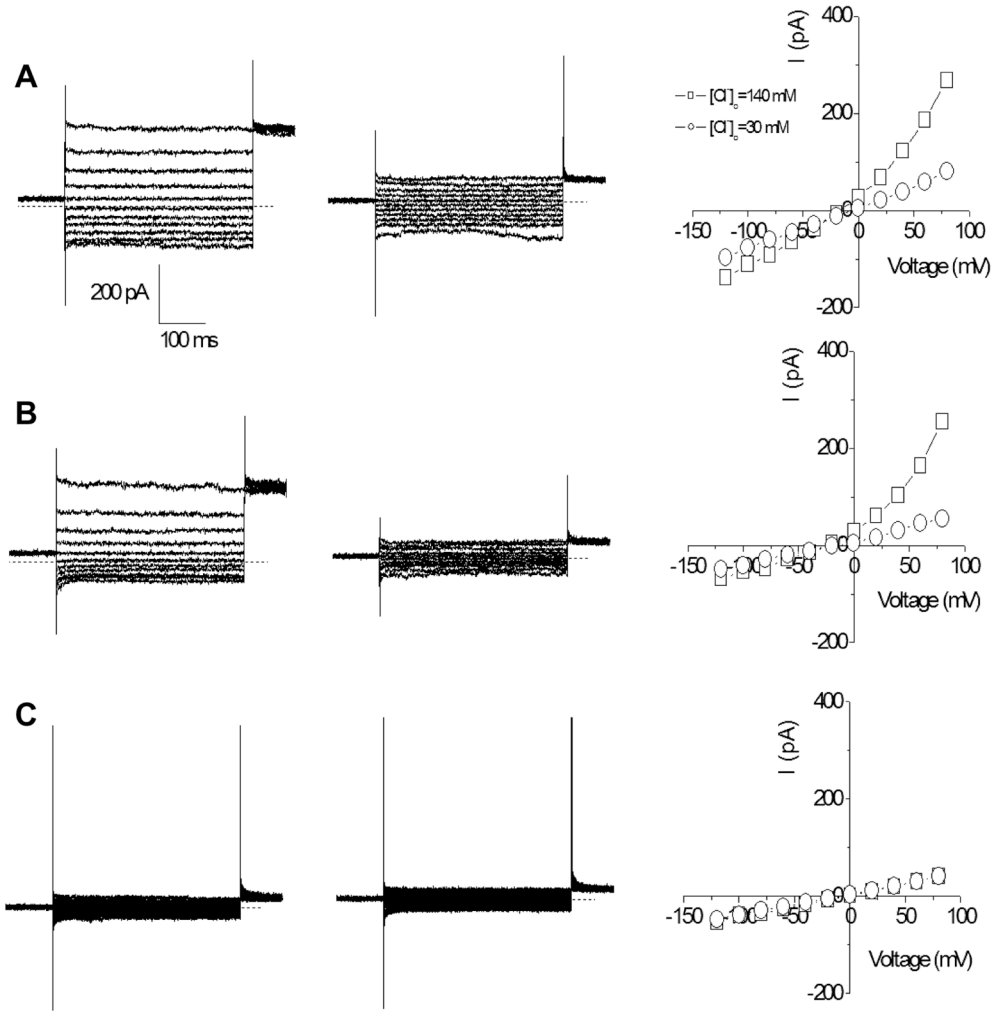

Figure 6. Chloride currents recorded in human corneal epithelial cells

Whole-cell chloride currents recorded from primary cultured human corneal epithelial cells (A), transformed HCE cells (B) and tsA201 cells as negative controls (C). The currents were recorded in bath solutions contained 140 mM Cl^- (left) or 30 mM Cl^- (middle). The current-voltage relationships are shown on the right. The zero current in the recordings are indicated by the dotted lines.

Table 1

PCR primers for detection of Chloride Channel and related genes on human corneal epithelium.

Gene name	Orientation	Start	Length	Tm	GC%	Sequence (5′->3′)	Product Size
CLC-1	FORWARD	656	20	59.87	45	GAATCCCCGAAATGAAGACA	201
	REVERSE	1584	20	60.07	50	TCCTACCAGCCTTCCAAATG	
CLC-2	FORWARD	1602	20	60.05	55	TCCTCACCCTGGTCATCTTC	402
	REVERSE	2003	20	59.88	55	GCAGGTAGGGCAGTTTCTTG	
CLC-3	FORWARD	909	20	60.06	50	GCACTGGCCGGATTAATAGA	401
	REVERSE	1309	20	60.14	55	GCCACAGCCAGGACTAATGT	
CLC-4	FORWARD	1359	20	59.99	55	CCCTGGTACATGGCTGAACT	203
	REVERSE	1561	20	60.13	55	CTCTGGCGTGTGTAGGGATT	
CLC-5	FORWARD	1475	20	59.99	55	TGGACTCCTCCAAGCTCTGT	178
	REVERSE	1652	20	60.04	50	AGGCCAGAAGGGATCTTCAT	
CLC-6	FORWARD	1111	20	59.97	45	ATTTGGGTTTCTTCGTCGTG	202
	REVERSE	1312	20	59.96	50	CGGCATTCTCCTAACACCAT	
CLC-7	FORWARD	1205	20	60.07	50	GGAGAAAATGGCCTACACGA	203
	REVERSE	1407	20	60.02	50	AGATCAGCACGAAGGCAACT	
CLC-KB	FORWARD	656	20	60.1	55	GTGATGATGGCTGCCTACCT	196
	REVERSE	851	20	59.92	55	CCCTCCAGTAATCCCAGACA	
CFTR	FORWARD	628	20	60.06	50	AAGCTGTCAAGCCGTGTTCT	401
	REVERSE	1028	20	59.99	55	GCCTTCCGAGTCAGTTTCAG	
ANO1	FORWARD	2636	20	59.98	50	TGTCAGAGCCAAAGACATCG	176
	REVERSE	2811	20	60.15	55	AGAGGGTGTGGTTGACGAAG	
CLC-C1	FORWARD	723	20	60.04	45	GCCAAGATGGAGCCATTAAA	200
	REVERSE	922	20	59.86	50	GGCTCCGTTACAAATGTGGT	
Keratin12	FORWARD	261	20	59.99	55	AGGACTGGGTGCTGGTTATG	398
	REVERSE	658	20	59.84	55	CAGCAGCTAGTCTCGCATTG	
Collagen 7	FORWARD	5900	20	60.01	55	TCTGGTAGCTTCCTGCCTGT	398
	REVERSE	6297	20	60.12	55	GGCTCATCCACAGACACCTT	
Collagen8	FORWARD	62	20	60.05	55	CACACGTTCACCAACTCACC	544
	REVERSE	605	20	59.96	50	TTGTTCCCCTCGTAAACTGG	